Received: 16 June 2017 | Revised: 3 January 2018 | Accepted: 12 March 2018

DOI: 10.1002/ptr.6089

RESEARCH ARTICLE

WILEY

Dehydroleucodine inhibits mitotic clonal expansion during adipogenesis through cell cycle arrest

S. Abood[1] | M. L. Veisaga[2] | L. A. López[3] | M. A. Barbieri[1,2,4,5]

[1] Department of Biological Sciences, Florida International University, Miami, FL 33199, USA

[2] Biomolecular Sciences Institute, Florida International University, Miami, FL 33199, USA

[3] Laboratory of Cytoskeleton and Cell Cycle, Institute of Histology and Embryology, Faculty of Medicine, National University of Cuyo, Mendoza 5500, Argentina

[4] Fairchild Tropical Botanic Garden, 10901 Old Cutler Road, Coral Gables, FL 33156, USA

[5] International Center of Tropical Botany, Florida International University, Miami, FL 33199, USA

Correspondence
M. A. Barbieri, Department of Biological Sciences, Florida International University, Miami, FL 33199, USA.
Email: barbieri@fiu.edu

Aberrant levels of preadipocyte differentiation, triggered by adipocyte hyperplasia and hypertrophy, results in the obesogenic phenotype. Obesity is a risk factor for several metabolic disorders. In this paper, dehydroleucodine inhibited the accumulation of lipid droplets and decreased the elevations of triglycerides, and this inhibitory effect occurred during the early stage of adipogenesis. Thus, not only did dehydroleucodine downregulate the expression of C/EBPα and PPARγ, it also strongly blocked the expression of C/EBPβ, an early stage biomarker of early adipogenesis, in a concentration-dependent manner. The proliferation of preadipocytes was dramatically suppressed when dehydroleucodine was added to the medium as early as 24 hr. These results indicate that dehydroleucodine may specifically affect mitotic clonal expansion to inhibit preadipocyte differentiation. Dehydroleucodine arrested the cell cycle at the G_0/G_1 phase, increased p27 and decreased both cyclins A and D and their partners (e.g., CDK2 and CDK4). Additionally, dehydroleucodine decreased phosphorylation of Erk1/2 and Akt. Furthermore, dehydroleucodine downregulated expression of histone demethylase JMJD2B as well as repressed the expression of histone methyltransferase MLL4, which in turn diminished the expression of C/EBPβ and PPARγ, respectively. Collectively, our results indicate that dehydroleucodine inhibits preadipocyte differentiation by blocking mitotic clonal expansion via cell cycle arrest, which may be mediated by regulation of selective histone methylation/demethylation in transcription activation during the early step of adipogenesis.

KEYWORDS

adipogenesis, C/EBPα, C/EBPβ, mitotic clonal expansion, PPARγ, sesquiterpene lactone

1 | INTRODUCTION

Ours is the first generation in the 200,000-year history of *Homo sapiens* where more members of our species are overweight and obese than underweight (Di Cesare et al., 2016). This sudden rise in global obesity prevalence from 105 million individuals in 1975 to 641 million in 2014 (Di Cesare et al., 2016) has coincided with a rise in a plethora of obesity related pathologies including cardiovascular disease (Florido et al., 2017), diabetes mellitus (Al-Goblan, Al-Alfi, & Khan, 2014), cancer (Zheng et al., 2017), stroke (R. Chen, Yan, Liu, Wang, & Wang, 2017), vascular dementia (Ilenia, Daniele, Michele, Enea, & Tayebati, 2017), and Alzheimer's disease (Ilenia et al., 2017). Although obesity is most commonly defined as a body mass index or BMI (body mass divided by the square of the body height) of over 30 kg/m^2, it is fundamentally characterized by an aberrant and excessive accumulation of adipose tissue due to adipocyte hyperplasia and hypertrophy (Muir et al., 2016).

These adipogenic processes can be modeled in vitro by utilizing a 3T3-L1 murine preadipocyte model system (Ruiz-Ojeda, Ruperez, Gomez-Llorente, Gil, & Aguilera, 2016), where cells are differentiated into mature adipocytes over the course of approximately 9 days through stimulation with an induction media (IM) cocktail consisting of growth media (GM) with dexamethasone, isobutylmethylxanthin

(IBMX), and insulin, in the first phase of differentiation, and GM with insulin alone in the second phase of differentiation. The transition to a mature adipogenic phenotype is evidenced by the accumulation of triglycerides (Rosen & Spiegelman, 2000), as well as the expression and/or phosphorylation of numerous genes including Akt1, Erk1/2, (Moon et al., 2007), the transcriptional factor peroxisome proliferator-activated receptor γ (PPARγ), and CCAAT/enhancer-binding proteins (C/EBPs).

C/EBPβ is expressed within 2 to 4 hr of treatment with IM and crucially acquires DNA binding activity at 12 hr post induction, which coincides with the essential process of mitotic clonal expansion (MCE). In this process cells undergo growth arrest followed by two to four rounds of mitosis, which is a necessary phase for the progression and completion of the adipocyte differentiation program (Tang, Otto, & Lane, 2003). C/EBPβ's DNA binding functionality is aided by retinoblastoma protein (Rb; P. L. Chen, Riley, Chen, & Lee, 1996). In contrast to Rb's role in negatively regulating transcription factor E2F-1 to prevent quiescent cells from passing a restriction point in G1, Rb binds with and activates C/EBPβ and does so specifically during the adipogenic differentiation process (P. L. Chen et al., 1996). MCE also requires a synchronized activation of the ERK and p38 signaling pathways (Aouadi et al., 2007; Tang et al., 2003). Progression from G1 to S requires downregulation of p27 and activation of CDK2 by cyclins E and A (Patel & Lane, 2000). Cyclin D1 and cyclin E are activated during the G_1 phase of the cell cycle (Choi et al., 2012). Once activated, cyclin D1 assembles with CDK4 or CDK6, or both, and cyclin E binds to CDK2 (Choi et al., 2012). Cyclins A and B are then recruited to CDK2 and CDK1, respectively, associations necessary for the inducement of cell cycle progression through S phase and mitosis (Choi et al., 2012). Activated C/EBPβ, along with C/EBPδ, triggers the expression of C/EBPα, which leads to the expression of PPARγ (Farmer, 2006). Once C/EBPβ is activated during MCE, it targets the promoter of the chromatin regulator gene *Kdm4b*, whereas C/EBPβ as a cofactor targets the promoters of cell cycle genes, including *Cdc45l* (cell division cycle 45 homolog) demethylates H3K9me3 in their regulatory regions, which in turn activates their transcription (Guo et al., 2012). *Cdc451* is a component of the CMG (CDC451 (protein), MCM (minichromosome maintenance), GINS (Sld5, Psf1, Psf2, and Psf3.)) complex, which is required for the initiation and elongation steps of eukaryotic chromosomal DNA replication (Tercero, Labib, & Diffley, 2000). Histone demethylase CDC25A is required for progression from G1 to the S phase of the cell cycle and acts by activating the pro-mitotic Cdc2 (CDK1) and also by activating G1/S cyclin-dependent kinases CDK4 and CDK2 by removing inhibitory phosphate groups from adjacent tyrosine and threonine residues (Goloudina et al., 2003). C/EBPβ also stimulates expression of histone H3K9 demethylase JMJD2B, which removes H3K9me3 and H3K9me2 on the promoters of PPARγ and C/EBPα, which stimulates their expression (Guo et al., 2012; Jang, Kim, & Jung, 2017). MLL3 and MLL4, H3K4me1/2 methyltransferases that become part of the activating signal cointegrator-2-containing complex (ASCOM), both redundantly coactivate PPARγ and C/EBPα (Lee et al., 2008). In opposition to these effects, histone methyltransferase G9a represses PPARγ expression by adding H3K9me2 to the entire PPARγ gene locus and promotes *Wnt10a* expression independent of its methyltransferase activity, therefore repressing adipogenesis (Wang et al., 2013).

Dehydroleucodine (DhL), a sesquiterpene lactone of the guaianolide group, which contains an α-methylene-γ-lactone ring, has been isolated from the aerial parts of *Artemisia douglasiana* (Giordano et al., 1990). Although DhL significantly inhibited the differentiation of 3T3-L1 preadipocytes in a time and concentration dependent manner by blocking the expression of PPARγ and C/EBPα (Galvis et al., 2011), the exact cellular and molecular mechanism by which DhL affected differentiation of 3T3-L1 preadipocytes is still not well understood. Interestingly, DhL inhibited proliferation and altered the cell cycle of cancer cells (Costantino et al., 2013). Therefore, it is possible that DhL affects the early stage of the differentiation of 3T3-L1 preadipocytes (i.e., MCE). The objective of this paper was to explore the effect of DhL on MCE during differentiation of 3T3-L1 preadipocytes, as well as elucidate aspects of the mechanism by which these effects occur.

2 | MATERIALS AND METHODS

2.1 | Reagents

3T3-L1 preadipocyte cells were purchased from the American Type Culture Collection (Manassas, VA). Dulbecco's Modified Eagle's Medium (DMEM), 1% penicillin/streptomycin, and 1% L-glutamine were purchased from Mediatech, Inc. (Manassas, VA). Ten percent fetal bovine calf serum was acquired from Invitrogen (Carlsbad, CA). Paraformaldehyde was purchased from Thermo Fisher Scientific Inc. (Pittsburgh, PA). Antibodies against PPARγ, C/EBPα, C/EBPβ, Cyclin A, Cyclin D1, CDK2, CDK4, p27, total (t)-Erk1/2, phospho (p)-Erk1/2, t-Akt1, p-Akt1, and GAPDH were obtained from Cell Signaling Technology (Beverly, MA). All secondary antibodies were purchased from Jackson ImmunoResearch Laboratories (West Grove, PA). DhL was isolated from *A. douglasiana* (voucher #37546, herbarium Mendoza Ruiz Leal, Instituto Argentino de Investigaciones de Zonas Aridas, Mendoza, Argentina) as previously described (Giordano et al., 1990). All other reagents, including insulin, IBMX, and dexamethasone, were obtained from Sigma-Aldrich unless otherwise stated. All chemicals were of analytical grade. A Triglyceride Quantification Kit was purchased from BioVision Research Products (Mountain View, CA).

2.2 | Cell culture and differentiation

3T3-L1 preadipoyctes were obtained from ATCC (Manassas, VA) and then grown to approximately 80% confluence, in a GM cocktail consisting of DMEM, 1% penicillin/streptomycin, 1% L-glutamine, and 10% fetal bovine serum. Cells were then differentiated in IM. Two recipes for the IM were employed during different times in the differentiation process. For the IM used during Days 1 and 3 of differentiation, GM was supplemented with 670-nM insulin (INS), 65-nM dexamethasone (DEX), and 0.5-mM 3-isobutyl-1-methylxanthine (IBMX). IM applied to the 3T3-L1 cells during Days 5, 7, and 9 of differentiation consisted of GM supplemented with 670 nM of insulin. Cells of passage nine or below were both grown to confluence and differentiated in a humidified atmosphere of a 5% CO_2 incubator at 37 °C.

2.3 | Cell viability assay

The MTT (3-[4,5-dimethylthiazol-2-yl]-2,5-diphenyl tetrazolium bromide) (Thermo Fisher Scientific. Inc., Pittsburgh, PA) colorimetric assay was utilized to quantify cellular viability. Cells (1×10^6 cells/ml) were incubated at 37 °C and 5% CO_2 in the absence or presence of different concentrations of DhL for various periods of time. After this initial incubation, cells were treated with MTT reagent at a final concentration of 5 mg/ml in phosphate buffer saline (PBS), and further incubated at 37 °C and 5% CO_2. Next, the formazan crystals were dissolved in a detergent reagent, and each condition was then quantified via spectrophotometry (Ultrospec 2100 Pro UV/Visible Spectrophotometer) at an optical density of 570 nm (OD_{570}) as described early (Barbieri, Fernandez-Pol, Hunker, Horazdovsky, & Stahl, 2004).

2.4 | Oil Red O Staining, microscopy, and spectrophotometry

After the 3T3-L1 preadipocytes were transferred from T75 flasks (where they were grown to approximately 80% confluence) to 12 well plates, GM was replaced with IM, and the cells underwent treatment with 9-μM DhL for different time periods in the differentiation process (Days 0–2, 2–4, 4–6, 6–8, and 0–8, respectively). On the 10th day of the differentiation program, the adipocytes were fixed with 4% paraformaldehyde solution in PBS for 1 hr at 4 °C. After fixing, cells were washed with 60% isopropanol and then stained with 0.3% Oil Red O solution for 45 min at room temperature. Cells were then washed twice with ddH_2O. The stained lipid droplets were visualized by light microscopy and photographed with a digital Leica DC 500 camera at 100× magnification. Images from 200 3T3-L1-control cells and 200 3T3-L1-DhL treated cells were examined. The size distribution of lipids droplets was analyzed by the NIH Image software, which can be accessed at the web site (http://rsb.info.nih.gov/nih-image/). For quantification of the lipid content, Oil Red O was eluted from cells by adding 100% isopropanol for 20 min and quantified by spectrophotometry at $OD_{540.}$

2.5 | Triglyceride assay

The lipid droplets in the cellular suspension were analyzed for total concentration of triglyceride as previously described (Mendez, Cabeza, & Hsia, 1986). Briefly, preadipocytes undergoing differentiation upon application of IM were treated with different concentrations of DhL for Days 0–2 and 0–8. Cells were washed with PBS, scraped, centrifuged, and lysed with 1% Triton X-100. Cell lysates were then centrifuged at 10,000× *g* for 20 min at 4 °C. Then, cell supernatants were used to measure the conversion of triglycerides to fatty acids and glycerol. DMSO was used as a vehicle control. The supernatants were then oxidized and quantified at OD_{540} based on a triglyceride standard curve (Cayman Chemical, Arbor, MI).

2.6 | Cell proliferation assay

3T3-L1 cells (5×10^4 cells/ml) were cultured in appropriate plates and then incubated with GM. When 3T3-L1 cells reached confluence, cells were incubated with IM in the absence or in the presence of various concentrations of DhL for 24 and 48 hr. DMSO was utilized as a vehicle control and preadipoyctes incubated in the absence of IM was used as a negative control. Cells were then harvested and quantified using an automated cell counter machine from Bio-Rad (Hercules, CA).

2.7 | Western blot analysis

After postconfluent preadipocytes were cultured in the absence or presence of IM and treated with 9-μM DhL for 10 min, 3 hr, or 24 hr, cell lystate preparation was conducted via the washing of cell monolayers with a mixture of ice-cold lysis buffer (20-mM Tris-HCL pH 7.5, 150-mM NaCl, 1% NP40, 1-mM Na_2 EDTA, and 0.1% Na Deoxycholate), protease inhibitors, and phosphatase inhibitors. After centrifugation, protein concentrations were quantified through the use of the BCA protein assay. Proteins were resolved by SDS-PAGE and transferred to nitrocellulose membranes (Thermo Fisher Scientific. Inc., Pittsburgh, PA), blocked in 5% bovine serum albumin overnight at 4 °C, and probed with the appropriate primary antibodies for 2 hr at room temperature. Membranes were next incubated with horseradish peroxidase-conjugated secondary antibodies overnight at 4 °C. Bands were visualized with enhanced chemiluminescence, and the intensities of the bands were quantified in WCIF Image J for Windows (University Health Network Research, Toronto, Canada), and relative levels of proteins were determined by densitometry analysis.

2.8 | Flow cytometry analysis

Cell cycle progression was measured by flow cytometric analysis after propidium iodide staining. Post confluence 3T3-L1 preadipocytes were incubated with IM in the absence or presence of 9-μM DhL for 24 hr. A suspension of cells were fixed with 70% ethanol at 4 °C and then incubated with propidium iodide staining buffer. Cells were analyzed with an Acurri-C6 Flow Cytometer (BD Biosciences, San Diego, CA), and cell cycle progression was measured with the Modfit LT program (Verity Software House, Topsham, ME).

2.9 | Real-time quantitative PCR

After selective treatment of 3T3-L1 cells with 9-μM DhL, RNA was extracted from 3T3-L1 cells by using RNeasy Plus Mini Kit (QIAGEN, USA) and cDNA library was synthesized by using iScript cDNA synthesis kit (BIO-RAD, USA) according to manufacturer's suggestion. Reverse transcription was performed with 200 ng of total RNA with reverse transcriptase in iScript reaction mix. Quantitative analysis of cDNA was performed using CFX96 Touch™ real-time Polymerase chain reaction (PCR) detection system (BIO-RAD, USA) and SsoAdvancedTM 227 universal probes supermix (BIO-RAD, USA) according to manufacturer's instruction. Briefly, amplification of the target cDNA was carried out with each 10-μL PCR mixtures containing cDNA, SSO probes, primers, and nuclease-free water. Target cDNA was amplified by using verified commercially available primer pairs (NM_007658.3 for CDC25A, NM_003504 for CDC451, NM_172132.2d for JMJD2B, NM_001081383.1 for MLL3, NM_001290573.1 for MLL4, NM_001289413.1 for G9A, NM_002046.5 for GAPDH, Mm00440940_m1 for PPARγ, and Mm00514283_s1 for C/EBPα, Thermo Fisher Scientific, USA). The conditions of PCR reaction were set

as follows: It started by the denaturation cycle at 95 °C for 30 min, and it was followed by incubation at 95 °C 10 min, and at 60 °C for 25 min, respectively. The mRNA expression was normalized to GAPDH. Relative gene expression was expressed as fold change in mRNA expression level compared with control.

2.10 | High-performance liquid chromatography

The SpectraSystem SMC1000 solvent delivery system, vacuum membrane degasser, P4000 gradient pumps, and AS3000 autosampler (Thermo Electro Corporation, San Jose, CA) were utilized for high-performance liquid chromatograhy. Column effluent was monitored at 254 nm (OD_{254}) with Spectra System UV6000LP variable wavelength PDA detector and ChromQuest 4.1 software. DhL was separated using a C18 YMC column, purified and identified as previously described (Galvis et al., 2011; Penissi, Piezzi, Villar, & Rudolph, 2003).

2.11 | Statistical analysis

All experiments were independently performed in triplicate. The standard error of the mean of triplicates was utilized and significance was analyzed by one-way ANOVA or Student's Test. All statistical data were from averages of the three independent experiments. Results with $^{*}p < .01$ and $^{**}p < .001$ were considered statistically significant.

3 | RESULTS

3.1 | DhL mostly inhibits early stages of adipocyte differentiation through attenuation of MCE

Previous studies have demonstrated that DhL and their epimers inhibited the differentiation of 3T3-L1 preadipocytes into adipocytes (Galvis et al., 2011). DhL structure is depicted in Figure 1a. Adipocyte differentiation occurs through the preadipocyte stages, which can be clearly divided into proliferation and mitotic cloning expansion (early state) and terminal differentiation (late stage; Ali, Hochfeld, Myburgh, & Pepper, 2013). Accordingly, we examined whether DhL causes stage-dependent inhibition of adipocyte differentiation. 3T3-L1 cells were treated with 9-μM DhL at several time points after induction with IM as shown in Figure 1b. We found that treatment with a single dose of DhL at early stages (days 0–2 and 2–4) significantly inhibited adipogenesis (Figure 1b). The treatment of DhL after day 4 (days 4–6 and 6–8) showed moderate inhibition of adipogenesis

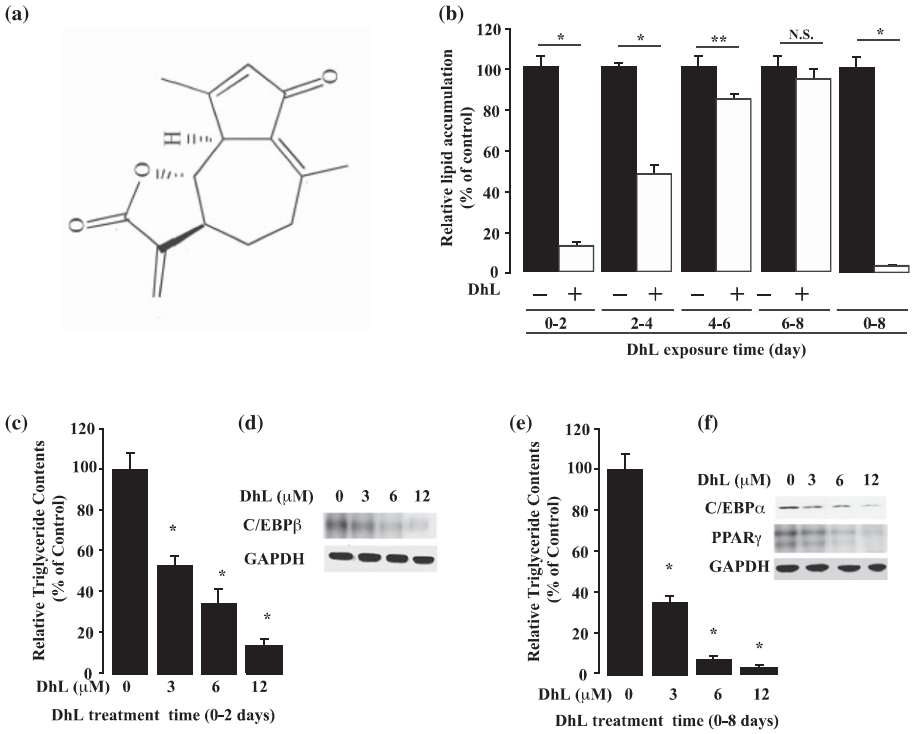

FIGURE 1 Inhibitory effect of dehydroleucodine on mitotic clonal expansion and on the expression of adipogenic transcriptional factors during early stage of adipogenesis. Preadipocytes were cultured in differentiation medium containing 9-μM DhL for several periods of time. (a) Chemical structure of DhL. (b) Preadipocytes were treated with DhL, and then cells were stained with Oil Red O and then visualized as described in Section 2. All values are presented as the mean ± SEM of three independent experiments performed in triplicate. $^{*}p < .01$ versus no DhL treatment. (c and e) Cellular triglyceride content of preadipocytes treated with different concentration of DhL for several periods of time as described in Section 2 using a Triglyceride Kit. Results are shown as relative percentage of control without DhL. DMSO was used a vehicle control. All values are presented as the mean ± SEM of three independent experiments performed in triplicate. $^{*}p < .01$ versus no DhL treatment. (f and g) Cells were incubated with DhL and harvested, and the lysates were subjected to Western blot analysis for PPARγ, C/EBPα, and C/EBPβ. GAPDH was used as a loading control. The Western blots were performed three times, and a representative image of the three independent experiments was shown

for days 4–6 (16 ± 2% of inhibition), whereas the treatment for days 6–8 showed no inhibition at all. As expected, the addition of DhL on Day 0 strongly inhibited differentiation of 3T3-L1 preadipocytes (Figure 1b). Consistent with these observations, when cells were treated with DhL during early stage (Days 0–2) or for the whole process (Days 0–8), the intracellular triglyceride content significantly decreased in a concentration-dependent manner (Figure 1c and 1e).

3T3-L1 preadipocytes undergo MCE through the upregulation of C/EBPβ and C/EBPδ during the early stage of adipocyte differentiation. This is followed by the activation of the downstream signaling molecules PPARγ and C/EBPα, which are critical for terminal adipocyte differentiation (Farmer, 2005). Therefore, we examined the effect of DhL on the expression of C/BEPβ, during the first 48 hr after stimulation of 3T3-L1 preadipocytes with IM. Expression of C/BEPβ was significantly decreased in a concentration-dependent manner when cells were treated with DhL (Figure 1d). In addition, PPARγ and C/EBPα expression in adipocytes treated with DhL strongly decreased compared with the control cells (Figure 1f). This was further evidenced in multiple experiments including the Oil Red O assays where both lipid droplet number and size were quantified after treatment with DhL. In these assays, both number of lipid droplets and size were reduced under all treatment conditions (Figure S1A).

3.2 | DhL inhibits MCE through downregulation of cyclins A and D and cyclin-dependent kinases 2 and 4

C/BEPβ, a specific transcriptional factor expressed in the early stage of adipogenesis, is also known to be required for MCE. Consequently, we determined whether DhL affects proliferation of 3T3-L1 preadipocytes after induction of differentiation with IM. As shown in Figure 2a, the treatment with DhL significantly decreased the cell numbers of IM-induced 3T3-L1 preadipocytes during Day 1 as well as Day 2 as compared with the cell numbers of control 3T3-L1 preadipocytes not treated with DhL. Furthermore, application of 3- and 6-μM DhL did not significantly affect 3T3-L1 preadipocyte cell viability. However, at 12.5-μM DhL concentration, preadipocyte number was decreased by 11 ± 3% as compared with untreated cells (Figure S1B). Thus, the

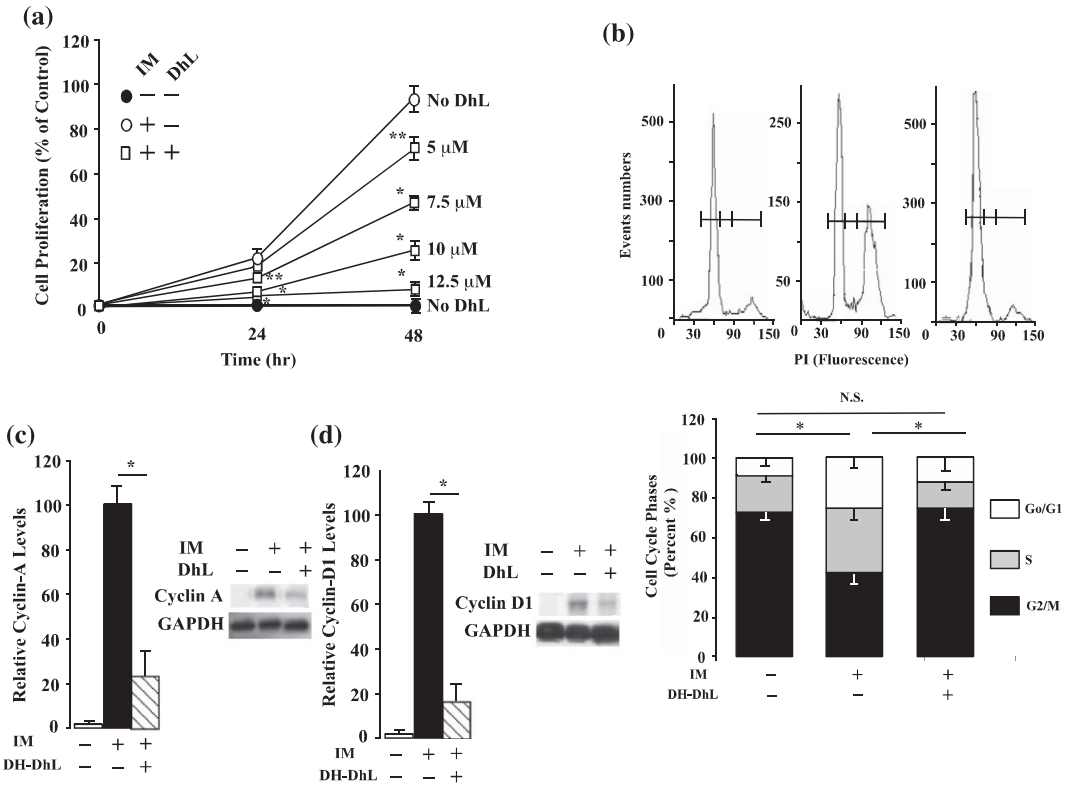

FIGURE 2 Dehydroleucodine inhibits proliferation and cell cycle progression of preadipocytes during mitotic clonal expansion. Postconfluent preadipocytes (Day 0) were cultured in differentiation medium and then treated once with different concentration of DhL as indicated. (a) The number of cells treated with different concentrations of DhL for 24 and 48 hr was determined using an automated cell counter machine. DMSO was used a vehicle control, and preadipocytes incubated in the absence of differentiation medium was used a negative control. All values are presented as the mean ± SEM of three independent experiments performed in triplicate. *$p < .01$, **$p < .001$ versus no DhL treatment. (b) After treatment of preadipocytes with 9-μM DhL for 24 hr, stained with a propidium iodide solution, and the cell population was analyzed by flow cytometry as described in Section 2. The percentage of cell population at each stage of the cell cycle was determined using Accuri C6 software. (c–h) After treatment of preadipocytes with 9-μM DhL for 24 hr, cells were harvested and the lysates were subjected to Western blot analysis for (c) Cyclin A, (d) Cyclin D1, (e) CDK2, (f) CDK4, and (g) p27. Western blot analysis for GAPDH was used as loading control. (h) Pre-adipocytes treated with 9-μM DhL for 10 min or 3 hr were harvested, and the lysates were subjected to Western blot analysis for total (t)-Erk1/2, t-Akt, phospho(p)-Erk1/2 and p-Akt. The Western blots were performed three times, and a representative image of the three independent experiments was shown

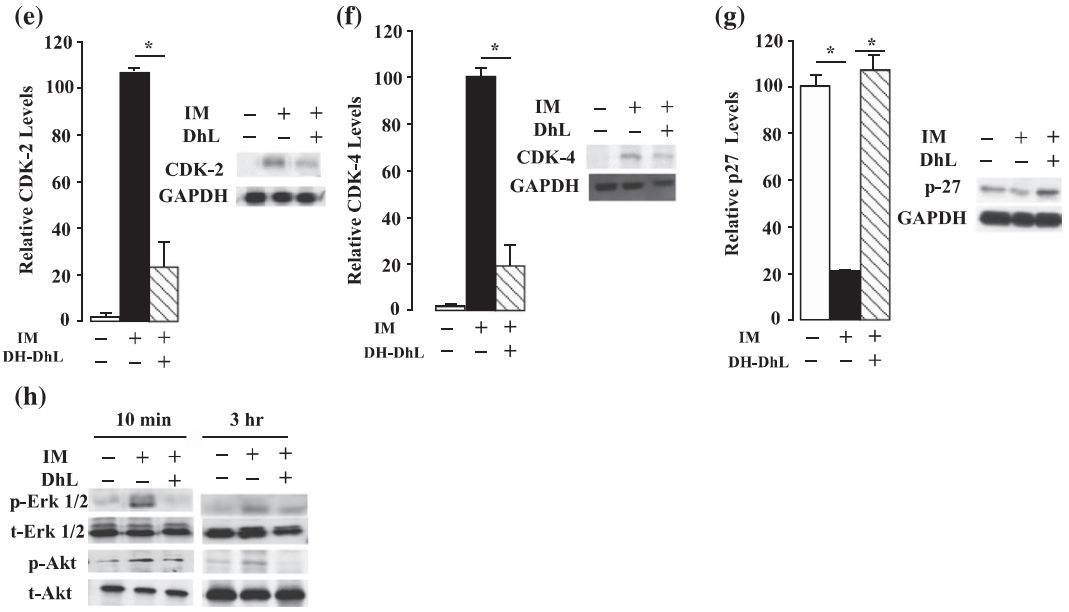

FIGURE 2 (Continued)

effects of DhL that cause inhibition of proliferation of 3T3-L1 preadipocytes appear to occur during the early stage of adipogenesis.

We then investigated whether DhL modulates cell cycle progression. When 3T3-L1 preadipocyte differentiation was induced, addition of DhL arrested the cell cycle at the G_0/G_1 phase (Figure 2b). Thepercentage of preadipocytes in the G_0/G_1 phase was about 71 ± 1.9% in the absence of IM, while 41 ± 2.5% in the presence of IM. Interestingly, 72 ± 3.1% of DhL-treated preadipocytes were in the G_0/G_1 phase. These observations indicated that DhL inhibited clonal expansion of the cell by inducing G_0/G_1 phase arrest. Cyclin D1, cyclin A, CDK2, and CDK4 are the cell cycle regulatory proteins at G_0/G_1 phase. When the preadipocytes were treated with 9-μM DhL, the expression of cyclin D1, cyclin A, CDK2, and CDK4 was strongly inhibited (Figure 2c–f). The expression of p27, an upstream effector of the cell cycle regulatory proteins, also decreased during adipogenesis but DhL restored its expression (Figure 2g). Interestingly, DhL also affected these key regulators of the cell cycle progression. These observations suggested that DhL induces cell cycle arrest at the G_0/G_1 phase through the upregulation of p27 expression, respectively.

To determine the signaling pathway through which DhL inhibited the clonal expansion during the early stage of adipogenesis, the expression and phosphorylation of Erk1/2 and Akt, which are involved in cell cycle progression, were examined. Adipogenic inducers increased the phosphorylation of Erk1/2 and Akt (Figure 2h). When the adipocytes were treated with 9-μM DhL for 10 min or 3 hr, both Erk1/2 and Akt phosphorylation was significantly decreased, but not to the level demonstrated for cyclin protein abundance.

3.3 | DhL blocks expression of C/EBPβ and PPARγ MCE

Several histone methyltransferases and demethylases have been reported to be involved in adipogenesis. These enzymes seem to regulate expression of C/EBPβ and PPARγ (Guo et al., 2012; Lee et al., 2008). To further assess the regulators involved in the DhL inhibition of MCE, we examined the expression of C/EBPβ in DhL-treated 3T3-L1 cells at the indicated time after IM induction as indicated in Figure 3. Level of expression of mRNA C/EBPβ was increased in the presence of IM treatment during the 18 hr. However, the addition of DhL clearly diminished the C/EBPβ mRNA level (Figure 3a), which expression has been correlated with the regulation of H3K9 demethylase JMJD2B and cell cycle genes (e.g., Cdc25c; Guo et al., 2012). Interestingly, protein expression of C/EBPβ was also decreased (Figure S2A). Thus, we determined the expression of JMJD2B and the cell cycle genes in DhL-treated 3T3-L1 cells during the MCE process. We observed that the JMJD2B mRNA level was also reduced by DhL treatment (Figure 3b). Interestingly, we also observed a dramatic inhibition of the expression of mRNA levels of cell cycle genes Cdc25A and Cdc451 during MCE (Figure 3c,d).

Then, we examined whether DhL affects the expression of PPARγ as well as methytransferases involved in its expression during adipogenesis. To this end, we determined the expression of MLL3, MLL4, and G9a in DhL-treated 3T3-L1 cells at the indicated time after IM induction. As shown in Figure 4, DhL clearly inhibited the expression of PPARγ and MLL4 (Figure 4a and 4c), without affecting the expression of MLL3 and G9a, respectively (Figure 4b and 4d). Consistent with these observations, DhL also repressed the expression of C/EBPα (Figure 1d) as well as PPARγ (Figure S2B). Interestingly, overexpression of C/EBPβ partially restored the inhibitory effect of DhL, suggesting that C/EBPβ function could be affected by DhL (compare lipid content of DhL-treated cells vs. DhL-treated overexpressing C/EBPβ; control cells: 100 ± 8%, DhL-treated cells: 20 ± 8%, C/EBPβ expressing cells: 135 ± 6%, C/EBPβ expressing DhL cells: 83 ± 7%; Figure S3). Thus, these results suggested that the DhL inhibition of MCE might be epigenetically regulated through downregulation of C/EBPβ and PPARγ.

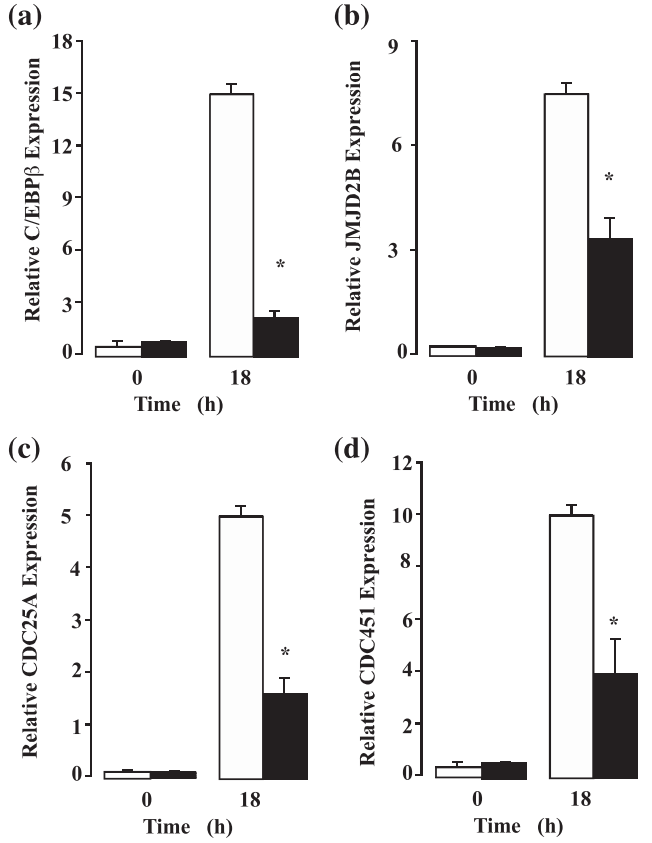

FIGURE 3 Dehydroleucodine downregulates the expression of C/EBPβ, histone demethylase JMJD2B, and CDC25A genes. Postconfluent preadipocytes (Day 0) were cultured in the presence of differentiation medium containing 9-μM DhL for 18 hr, then total RNA was extracted as indicated in Section 2. (a–d) mRNA levels of (a) C/EBPβ, (b) histone demethylase JMJD2B, (c) CDC25A, and (d) CDC451 were determined by qPCR. The qPCR data are represented as the mean ± SEM of there independent experiments. *p < .01 versus no DhL treatment

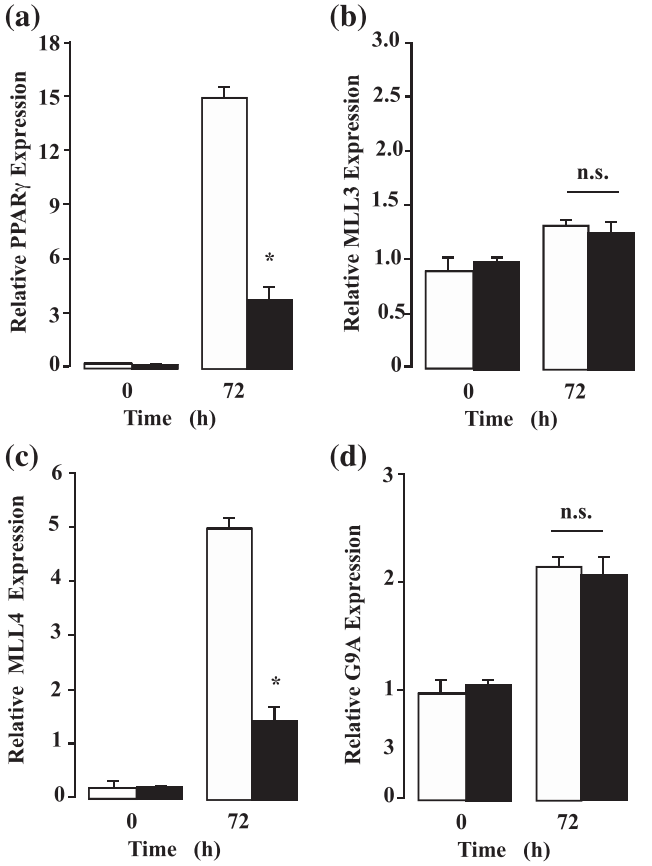

FIGURE 4 Dehydroleucodine represses the expression of PPARγ, MLL3, MLL4, and G9A genes. Postconfluent preadipocytes (Day 0) were cultured in the presence of differentiation medium containing 9-μM DhL for 72 hr, and then total RNA was extracted as indicated in Section 2. (a–d) mRNA levels of PPARγ, MLL3, MLL4, and G9A were determined by qPCR. The qPCR data are represented as the mean ± SEM of there independent experiments. *p < .01 versus no DhL treatment, and N.S.: no statistically significant as compared with no DhL treatment

3.4 | Stability, absorption, and bioavailability of DhL

The stability of drugs in both solid and liquid states are affected not only by their chemistry but also by their environment, such as ambient temperature, moisture content, light, and their surrendering. Thus, evaluation of DhL, as any guaianolide sesquiterpene lactone, should begin with an examination of chemical structure, which provides some indication of chemical reactivity because this compound contains several groups that can suffer intermolecular cyclization, hydrolysis, and oxidization (Cordell, 1976).

In Figure S4A, the pH of solution has a dramatic effect on DhL stability in liquid state. DhL is comparatively stable when the environmental pH is in the range of 5 to 7, becoming unstable when pH is less than 3 or more than 7.

In Figure S4B, DhL (in solid stage) content remains constant for 40-day storage in a refrigerator (4 °C). At 25 and 37 °C, DhL begins to degrade slowly after 30 days. We only observed 3 ± 2% and 5 ± 1% degradation, respectively. However, DhL degradation can reach 17 ± 5% after 40-day storage at 50 °C.

The bioavailability and uptake of DhL were determined using Caco-2 as well as in 3T3-L1 cells as essentially described early (Walle, Galijatovic, & Walle, 1999). In Caco-2 cells, the permeability coefficient and percent transport of DhL at a concentration of 200 μM were determined in the apical part of the monolayer. Transport of DhL was observed with permeability coefficient value of 10.06×10^{-6} cm/s and a percent transport of 26.31 ± 0.71%. The cumulative amount transported was linear with time, and it was monitored for a period of 3 hr. Moreover, in 3T3-L1 cells, the cumulative amount transported was also linear with time (Figure S4C).

4 | DISCUSSION

Approximately 50% of modern pharmaceuticals derived from traditional plant compounds (Bilia et al., 2017). A deeper understanding of the antiadipogenic mechanism of action of the sesquiterpene lactone DhL, derived from *A. douglasiana*, may thus have pharmacological importance in the continuing search for therapeutic modalities to ameliorate the effects of the global obesity epidemic. The aim of this study was to advance the elucidation of the potential mechanisms of action of DhL, that previous work revealed acts upon middle stage, and possibly late stage, differentiation of 3T3-L1 preadipocytes (Galvis et al., 2011).

It is evident from the results of our study that DhL has a multiplicity of effects on adipogenesis and therefore is likely that DhL interacts with multiple molecular actors and/or acts upstream of significant processes responsible for the progression of signaling cascades necessary for MCE. Our study established that DhL has a marked effect on lipid accumulation when applied to 3T3-L1 cells between 0 and 2 days post induction of differentiation (Figure 1b). When applied from Day 4 through Day 8 post induction, the antiadipogenic affect was drastically reduced (Figure 1b), indicating that one single dose of DhL acts by inhibiting the early stage of adipogenesis, during which MCE occurs. Results from a triglyceride assay confirmed these findings, demonstrating that within this 0- to 2-day postinduction period, several concentrations of DhL effectively decreased triglyceride content, an observable marker of successful progression through the adipogenic program (Figure 1c). This decreased triglyceride content was still observed when low concentrations of DhL (3 and 6 μM) were applied (Figure 1e).

C/EBPβ is expressed within 2 to 4 hr post induction (Tang et al., 2003), and we observed in this study that 3 and 6 μM of DhL led to a drastic downregulation of protein levels of C/EBPβ (Figure 1d). As the acquisition of DNA binding activity of C/EBPβ beginning at approximately 12 hr post induction is essentially required for the progression of MCE (Tang et al., 2003), this represents strong evidence that DhL inhibits adipogenesis by obstructing the MCE process. As activated C/EBPβ, along with C/EBPδ, triggers the expression of C/EBPα, which leads to the expression of PPARγ (Farmer, 2006), the inhibitory effects of DhL on C/EBPβ would be expected to result in a downreguation of protein levels of PPARγ and C/EBPα. This is precisely what was observed when increasing concentrations of DhL (at 3, 6, 12 μM, and beyond) was applied in our study, which drastically downregulated PPARγ and C/EBPα in an inversely correlated manner (Figure 1f).

Both MAPK and PI3K/Akt pathways affect mitogenic signaling molecules via activation of C/EBPβ, as well as cell cycle progression through regulation of cyclin D and p27 expression. Cyclin D and p27 expression induce adipocyte differentiation (Aouadi et al., 2007; Tang et al., 2003). Flow cytometry revealed that DhL arrested the cell cycle at the G_0/G_1 phase (Figure 2b), decreased both cyclins A and D1 and their partners (CDK2 and CDK4; Figure 2c–f), and increased p27 (Figure 2g). Consistent with this arresting of cell cycle progression, DhL inhibited the proliferation of preadipocytes during MCE in a concentration dependent manner with the greatest effect observed at 12.5 μM of DhL (Figure 2a). Expression of CDK inhibitor p27 was downregulated during adipogenesis, but DhL restored its expression as shown in Figure 2g. DhL also decreased phosphorylation of Erk1/2 and Akt (Figure 2h), whose activities have been associated with stimulation of adipogenesis. Thus, the results suggest that DhL may induce cell cycle arrest at G0/G1 via its actions upon Erk1/2 and Akt, as well as via its upregulation of p27.

DhL also repressed the expression of CDC25A, CDC451, and JMJD2B (Figure 3), which all act downstream of C/EBPβ to facilitate progression through the cell cycle (Aressy & Ducommun, 2008; Guo et al., 2012; Turowski et al., 2003). mRNA levels of the H3K4me1/2 methyltransferase MLL4 were downregulated upon application of DhL (Figure 4c), and PPARγ mRNA was also downregulated, as would be expected from the literature reporting that MLL4 is part of the ASCOM, which coactivates PPARγ (Lee et al., 2008). No significant effects were found on mRNA levels upon application of DhL for the expression of MLL3 (Figure 4b), also a part of the ASCOM (Lee et al., 2008), or the expression of G9A (Figure 4d), which represses PPARγ expression (Wang et al., 2013).

It is plausible that this multitude of effects, which arrest the necessary step of MCE, stem from the upstream inhibitory effect DhL may have on C/EBPβ function. Alternatively, DhL could also affect factors necessary to express C/EBPβ or activate C/EBPβ's DNA binding activity. Such targets could possibly include Rb, which DhL decreased phosphorylation of Rb in this study (Barbieri, M. A., personal communication October 23, 2017), and which binds to C/EBPβ and facilitates its activation (P. L. Chen et al., 1996). It is also possible that DhL acts redundantly and directly on numerous processes downstream of C/EBPβ activation, such as obstructing MLL4, which was downregulated in this study (Figure 4c). MLL3 and MLL4 are part of the ASCOM, which are integral to the activation of PPARγ and C/EBPα (Lee et al., 2008). DhL could possibly exert its antiadipogenic effects by acting upon C/EBPβ rather than the ASCOM. In a similar fashion, DhL may act directly on the epigenetic modifiers as shown in this study, which include CDC25A, CDC45l, and JMJD2B (Figure 3b–d). Further studies can better clarify these mechanistic issues where DhL could be considered as an agent with either a more generic or specific antiadipogenic activity.

We also examined the stability, absorption, and bioavailability of the DhL in our study. Clearly, the stability of DhL is affected in different environment aqueous solution, suggesting that hydrolysis may be the predominant degradation pathway of DhL solution that is subject to specific-acid and specific-base catalyzers. In solid, state of DhL (i.e., dry powder), which contained very limited amount of water, makes its degradation highly unlikely even at temperature more than 37 °C for the period of time examined. Interestingly, the data on permeability of DhL can be compared with a representative model compound (i.e., propranolol) for absorption. Propranolol is a cellular transport marker, which is highly lipophilic, and exhibits a high value of permeability coefficient (i.e., 14.8×10^{-6}; Chong, Dando, & Morrison, 1997). The permeability coefficient value of DhL observed in our study is lower than that of propranolol but higher than parthenolide (Khan, Abourashed, Khan, & Walker, 2003); hence, DhL could be in the category of moderate to high absorption.

To further characterize the potential efficacy of DhL, preliminary pharmacologic studies were indicate that an i.p. DhL dose of 50 mg/kg reached a concentration maximum (C_{max}) of 12.7 μM and a half-life ($T_{1/2}$) of 47 min in serum. In addition, oral bioavailability was approximately 66% compared with i.p. administration. Furthermore, in preliminary toxicology studies, daily administration of 50 mg/kg DhL to mice for 5 consecutive days was well tolerated (Barbieri, M. A., manuscript in preparation), which is consistent with previous observations that DhL is well tolerated in rodents (Costantino et al., 2016; Penissi, Giordano, Guzmán, Rudolphd, & Piezzi, 2006).

This study has elucidated some of the early mechanistic effects of DhL-facilitated adipogenic inhibition during the early stage process of MCE. We hope that it will lead to future studies to further investigate its antiadipogenic mechanism during MCE that may lead to translational efforts to ameliorate our current obesity situation.

ACKNOWLEDGEMENT

The authors are grateful to Dr. David Lee and Dr. Barbieri laboratory's members for their insightful comments.

CONFLICT OF INTEREST

The authors have declared that there is no conflict of interest.

ORCID

M. A. Barbieri http://orcid.org/0000-0002-3002-1318

REFERENCES

Al-Goblan, A. S., Al-Alfi, M. A., & Khan, M. Z. (2014). Mechanism linking diabetes mellitus and obesity. *Diabetes, Metabollic Syndrome and Obesity*, *7*, 587–591.

Ali, A. T., Hochfeld, W. E., Myburgh, R., & Pepper, M. S. (2013). Adipocyte and adipogenesis. *European Journal of Cell Biology*, *92*, 229–236.

Aouadi, M., Jager, J., Laurent, K., Gonzalez, T., Cormont, M., Binétruy, B., … Bost, F. (2007). p38MAP Kinase activity is required for human primary adipocyte differentiation. *FEBS Letters*, *581*, 5591–5596.

Aressy, B., & Ducommun, B. (2008). Cell cycle control by the CDC25 phosphatases. *Anti-Cancer Agents in Medicinal Chemistry*, *8*, 818–824.

Barbieri, M. A., Fernandez-Pol, S., Hunker, C., Horazdovsky, B. H., & Stahl, P. D. (2004). Role of rab5 in EGF receptor-mediated signal transduction. *European Journal of Cell Biology*, *83*, 305–314.

Bilia, A. R., Piazzini, V., Guccione, C., Risaliti, L., Asprea, M., Capecchi, G., & Bergonzi, M. C. (2017). Improving on nature: The role of nanomedicine in the development of clinical natural drugs. *Planta Medica*, *83*, 366–381.

Chen, P. L., Riley, D. J., Chen, Y., & Lee, W. H. (1996). Retinoblastoma protein positively regulates terminal adipocyte differentiation through direct interaction with C/EBPs. *Genes & Development*, *10*, 2794–2804.

Chen, R., Yan, J., Liu, P., Wang, Z., & Wang, C. (2017). Plasminogen activator inhibitor links obesity and thrombotic cerebrovascular diseases: The roles of PAI-1 and obesity on stroke. *Metabolic Brain Disease*, *32*, 667–673.

Choi, K. M., Lee, Y. S., Sin, D. M., Lee, S., Lee, M. K., Lee, Y. M., … Yoo, H. S. (2012). Sulforaphane inhibits mitotic clonal expansion during adipogenesis through cell cycle arrest. *Obesity (Silver Spring)*, *20*, 1365–1371.

Chong, S., Dando, S. A., & Morrison, R. A. (1997). Evaluation of Biocoat intestinal epithelium differentiation environment (3-day cultured Caco-2 cells) as an absorption screening model with improved productivity. *Pharmaceutical Research*, *14*, 1835–1837.

Cordell, G. A. (1976). Biosynthesis of sesquiterpenes. *Chemical Reviews*, *76*, 425–460.

Costantino, V. V., Lobos-Gonzalez, L., Ibañez, J., Fernandez, D., Cuello-Carrión, F. D., Valenzuela, M. A., … Lopez, L. A. (2016). Dehydroleucodine inhibits tumor growth in a preclinical melanoma model by inducing cell cycle arrest, senescence and apoptosis. *Cancer Letters*, *372*, 10–23.

Costantino, V. V., Mansilla, S. F., Speroni, J., Amaya, C., Cuello-Carrión, D., Ciocca, D. R., … Lopez, L. A. (2013). The sesquiterpene lactone dehydroleucodine triggers senescence and apoptosis in association with accumulation of DNA damage markers. *PLoS One*, *8*, e53168.

Di Cesare, M., Bentham, J., Stevens, G. A., Zhou, B., Danaei, G., Lu, Y., … Cisneros, J. Z. (2016). Trends in adult body-mass index in 200 countries from 1975 to 2014: A pooled analysis of 1698 population-based measurement studies with 19.2 million participants. *Lancet*, *387*, 1377–1396.

Farmer, S. (2005). Regulation of PPARγ activity during adipogenesis. *International Journal of Obesity*, *29*, S13–S16.

Farmer, S. R. (2006). Transcriptional control of adipocyte formation. *Cell Metabolism*, *4*, 263–273.

Florido, R., Ndumele, C. E., Kwak, L., Pang, Y., Matsushita, K., Schrack, J. A., … Selvin, E. (2017). Physical activity, obesity, and subclinical myocardial damage. *JACC Heart Failure*, *5*, 377–384.

Galvis, A., Marcano, A., Stefancin, C., Villaverde, N., Priestap, H. A., Tonn, C. E., … Barbieri, M. A. (2011). The effect of dehydroleucodine in adipocyte differentiation. *European Journal of Pharmacology*, *671*, 18–25.

Giordano, O. S., Guerreiro, E., Pestchanker, M. J., Guzman, J., Pastor, D., & Guardia, T. (1990). The gastric cytoprotective effect of several sesquiterpene lactones. *Journal of Natural Products*, *53*, 803–809.

Goloudina, A., Yamaguchi, H., Chervyakova, D. B., Appella, E., Fornace, A. J. Jr., & Bulavin, D. V. (2003). Regulation of human Cdc25A stability by Serine 75 phosphorylation is not sufficient to activate a S phase checkpoint. *Cell Cycle*, *2*(5), 473–478.

Guo, L., Li, X., Huang, J. X., Huang, H. Y., Zhang, Y. Y., Qian, S. W., … Tang, Q. Q. (2012). Histone demethylase Kdm4b functions as a co-factor of C/EBPbeta to promote mitotic clonal expansion during differentiation of 3T3-L1 preadipocytes. *Cell Death and Differentiation*, *19*, 1917–1927.

Ilenia, M., Daniele, T., Michele, M., Enea, T., & Tayebati, S. K. (2017). Obesity and metabolic syndrome affects the cholinergic transmission and cognitive functions. *CNS & Neurological Disorders Drug Targets*. https://doi.org/10.2174/1871527316666170428123853

Jang, M. K., Kim, J. H., & Jung, M. H. (2017). Histone H3K9 Demethylase JMJD2B Activates Adipogenesis by Regulating H3K9 Methylation on PPARγ and C/EBPα during Adipogenesis. *PLoS One*, *12*, e0168185.

Khan, S. I., Abourashed, E. A., Khan, I. A., & Walker, L. A. (2003). Transport of Parthenolide across Human Intestinal Cells (Caco-2). *Planta Medica*, *69*, 1009–1012.

Lee, J., Saha, P. K., Yang, Q. H., Lee, S., Park, J. Y., Suh, Y., … Lee, J. W. (2008). Targeted inactivation of MLL3 histone H3-Lys-4 methyltransferase activity in the mouse reveals vital roles for MLL3 in adipogenesis. *Proceedings of the National Academy of Sciences of the United States of America*, *105*, 19229–19234.

Mendez, A. J., Cabeza, C., & Hsia, S. L. (1986). A fluorometric method for the determination of triglycerides in nanomolar quantities. *Analytical Biochemistry*, *156*, 386–389.

Moon, H. S., Chung, C. S., Lee, H. G., Kim, T. G., Choi, Y. J., & Cho, C. S. (2007). Inhibitory effect of (-)-epigallocatechin-3-gallate on lipid accumulation of 3T3-L1 cells. *Obesity (Silver Spring)*, *15*, 2571–2582.

Muir, L. A., Neeley, C. K., Meyer, K. A., Baker, N. A., Brosius, A. M., Washabaugh, A. R., … O'Rourke, R. W. (2016). Adipose tissue fibrosis, hypertrophy, and hyperplasia: Correlations with diabetes in human obesity. *Obesity (Silver Spring)*, *24*, 597–605.

Patel, Y. M., & Lane, M. D. (2000). Mitotic clonal expansion during preadipocyte differentiation: Calpain-mediated turnover of p27. *The Journal of Biological Chemistry*, *275*, 17653–17660.

Penissi, A. B., Giordano, O. S., Guzmán, J. A., Rudolphd, M. I., & Piezzi, R. S. (2006). Chemical and pharmacological properties of dehydroleucodine, a lactone isolated from Artemisia douglasiana Besser. *Molecular Medicinal Chemistry*, *10*, 1–11.

Penissi, A. B., Piezzi, R. S., Villar, M., & Rudolph, M. I. (2003). A new high-performance liquid chromatography method for the determination of dehydroleucodine in plant extracts. *Chromatographia*, *58*, 659–664.

Rosen, E. D., & Spiegelman, B. M. (2000). Molecular regulation of adipogenesis. *Annual Review of Cell and Developmental Biology*, *16*, 145–171.

Ruiz-Ojeda, F. J., Ruperez, A. I., Gomez-Llorente, C., Gil, A., & Aguilera, C. M. (2016). Cell models and their application for studying adipogenic differentiation in relation to obesity: A review. *International Journal of Molecular Sciences*, *17*. https://doi.org/10.3390/ijms17071040

Tang, Q. Q., Otto, T. C., & Lane, M. D. (2003). Mitotic clonal expansion: A synchronous process required for adipogenesis. *Proceedings of the National Academy of Sciences of the United States of America*, *100*, 44–49.

Tercero, J. A., Labib, K., & Diffley, J. F. (2000). DNA synthesis at individual replication forks requires the essential initiation factor Cdc45p. *The EMBO Journal*, *19*, 2082–2093.

Turowski, P., Franckhauser, C., Morris, M. C., Vaglio, P., Fernandez, A., & Lamb, N. J. (2003). Functional cdc25C dual-specificity phosphatase is

required for S-phase entry in human cells. *Molecular Biology of the Cell*, *14*, 2984–2998.

Walle, U. K., Galijatovic, A., & Walle, T. (1999). Transport of the flavonoid chrysin and its conjugated metabolites by human intestinal cell line Caco-2. *Biochemical Pharmacology*, *58*, 431–438.

Wang, L., Xu, S., Lee, J. E., Baldridge, A., Grullon, S., Peng, W., & Ge, K. (2013). Histone H3K9 methyltransferase G9a represses PPARγ expression and adipogenesis. *The EMBO Journal*, *32*, 45–59.

Zheng, J., Zhao, M., Li, J., Lou, G., Yuan, Y., Bu, S., & Xi, Y. (2017). Obesity-associated digestive cancers: A review of mechanisms and interventions. *Tumour Biology*, *39*. 1010428317695020 doi: https://doi.org/10.1177/1010428317695020

SUPPORTING INFORMATION

Additional Supporting Information may be found online in the supporting information tab for this article.

How to cite this article: Abood S, Veisaga ML, López LA, Barbieri MA. Dehydroleucodine inhibits mitotic clonal expansion during adipogenesis through cell cycle arrest. *Phytotherapy Research*. 2018;32:1583–1592. https://doi.org/10.1002/ptr.6089